JOURNAL OF APPLIED POLYMER SCIENCE VOL. 17, PP. 3637–3650 (1973)

On the Dynamics of Melt Spinning

E. CERNIA, *Istituto di Chimica Industriale, Università di Roma, Rome, Italy,* and W. CONTI, *SNAM PROGETTI S.p.A., Direzione Generale Ricerca e Sviluppo, S. Donato Milanese, Milan, Italy*

Synopsis

The dynamics of melt spinning was examined in the case of a Lethersich liquid taking also into account a phenomenologic way as well the transition zone between shear and elongational flow. The shape of the fluid jet was measured under many spinning conditions; the filament temperature and the fluid viscosity were then calculated. The experimental viscosity temperature relationship was compared with the W. L. F. equation, and the comparison makes it clear that the Newtonian model is not adequate whereas all the experimental evidence is in qualitative accordiance with the proposed model.

INTRODUCTION

The physical characteristics of man-made fibers are a result of several technological operations including spinning, drawing, heat treating, etc. The structure of the "as spun" fibers, i.e., the filament after the spinning process, is of great importance on the control of the drawing process and (indirectly) on the physical properties of finished fibers.[1] Moreover, the structure of the "as spun" fibers depends on the spinning conditions. For this reason, many authors have studied the rheology, dynamics, and solidification of the fluid jet during the spinning process.[1,2]

From the rheological point of view, any spinning process can be divided into three steps: (i) shear flow of the spinning fluid within the spinneret channel, (ii) transition zone between shear and elongational flow; in this zone the fluid polymer can increase its diameter (die swell or Barus effect), and (iii) elongation of the fluid jet under the external tensile force applied by the winding-up device. The fluid jet is tranformed into a solid fiber during the two last steps.

It is a common opinion that in the fiber-spinning process the memory of the flow into the spinneret has no importance; i.e., the rate of solidification is lower than the reciprocal relaxation time of the molecular orientation developed into the spinneret. In this case, the dynamics and the kinematics of the spinning process can be developed without any reference to the memory of the orientation during the extrusion.

The shape of the fluid polymer jet in the steady-state melt-spinning process can be theoretically predicted under any given spinning conditions.

An exact solution of this problem would require consideration of the simultaneous system of differential equations involving force balance, heat transfer, constitutive rheological equation, and expression for heat transfer coefficient and temperature-dependent rheological parameters.

A very important simplification for the resolution of this problem comes from the hypothesis of a uniform deformation of the cross section; in fact, the hydrodynamics equations and the heat transfer equation can be independently solved. In the case of Newtonian fluid, there is a further important simplification. With these main and other less substantial hypotheses, it is possible to calculate the temperature[3] and the Newtonian viscosity from the shape of the fluid jet.[4] However, the flow activation energy calculated in such a way is too low[4] to be accepted.

In the present paper, we shall try to solve the problem in the case of a Lethersich liquid,[5] taking into account also the transition zone in a phenomenologic way as well. It follows that the effects of the memory of flow conditions prior to entry into the spinneret and in the spinneret as well are considered.

STATEMENT OF PROBLEM

Two antagonistic effects are present in the transition zone between shear and elongational flow. The jet emerging from the spinneret increases its diameter because of the Barus effect and decreases the diameter owing to the wind-up speed. According to the well-known equation for the parallel velocity gradient ($\dot{\gamma}$) in the fluid jet,[4]

$$\dot{\gamma} = -\frac{q}{S(x)} \frac{d \ln S(x)}{dx} \tag{1}$$

where q is the constant rate of flow and $S(x)$ is the jet cross section at a distance x from the spinneret, we see that γ is negative as long as the diameter increases.

This velocity gradient can be considered to comprise two components: the first one ($\dot{\gamma}_f$) connected with the elongational flow, and the second one ($-\dot{\gamma}_r$) caused by the Barus effect. That is,

$$\dot{\gamma} = \dot{\gamma}_f - \dot{\gamma}_r$$

or, for convenience,

$$\dot{\gamma} = \dot{\gamma}_f(1 - f) \tag{2}$$

where $f = \dot{\gamma}_r/\dot{\gamma}_f$. The value of f and its time derivatives will be dependent on the extrusion conditions and on the rheological properties of the fluid.

From a phenomenological point of view, we can suppose that the swelling will develop according to a characteristic time parameter (τ^*) dependent on the time owing to the nonisothermal conditions along the spinning line; in this case we have

$$\frac{df}{dt} + \frac{1}{\tau^*} f = 0.$$

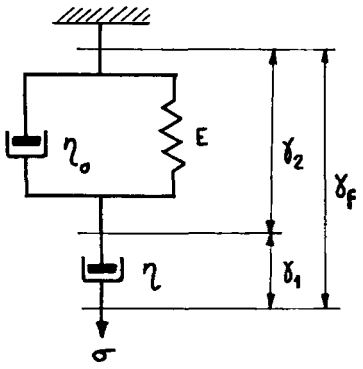

Fig. 1. Lethersich model.

The previous equation yields

$$f = f_0 \exp\left(-\int_0^t \frac{dt'}{\tau^*}\right)$$

where the f_0 value will depend on the extrusion conditions and the fluid properties. The previous equation can assume a more suitable form by means of the following relationship:

$$dt = \frac{dx}{v(x)} = \frac{1}{q} S(x)dx$$

where $v(x)$ is the velocity of the fluid jet at a distance x from the spinneret. Since

$$y^* = \int_0^x \frac{S(x')}{\tau^*} dx'$$

we have

$$f = f_0 \exp\,(-y^*(x)/q).$$

Substituting the previous equation into the eq. (2), we obtain

$$\dot{\gamma} = \dot{\gamma}_f\left[1 - f_0 \exp\left(-\frac{y^*}{q}\right)\right]. \tag{3}$$

We shall now consider that the fluid jet can be described by a Lethersich fluid (Fig. 1) where the parameters E (elastic modulus) and η and η_0 (viscosities) are dependent on the temperature and consequently dependent on the time or on the distance x. The rate of deformation (or the parallel velocity gradient) of the Lethersich fluid ($\dot{\gamma}_f$) is given by the sum of the rate of deformation of the viscous element ($\dot{\gamma}_1$) with that of the Kelvin viscoelastic element ($\dot{\gamma}_2$). Both rates of deformation are correlated with the local stress (σ) by the following differential equations:

$$\eta\dot{\gamma}_1 = \sigma$$

$$\eta_0\dot{\gamma}_2 + E\gamma_2 = \sigma.$$

From the previous equations we can easily get $\dot{\gamma}_1$ and $\dot{\gamma}_2$, so that we have the following equation (expressed in axial distance x instead of time):

$$\dot{\gamma}_f = \dot{\gamma}_1 + \dot{\gamma}_2 = \sigma\left(\frac{1}{\eta} + \frac{1}{\eta_0}\right) - \tau \exp\left(-\frac{y}{q}\right)\int_0^x \frac{\sigma}{\eta_0} \exp\left(\frac{y}{q}\right) dx' \quad (4)$$

where

$$\tau = \eta_0/E \qquad y = \int_0^x \frac{S(x')}{\tau}\, dx'.$$

The stress $\sigma = F(x)/S(x)$ is dependent on x not only because the cross section $S(x)$ is x dependent, but also because the tractional force $F(x)$ is x dependent. In fact, $F(x)$ is the resultant force of some x-dependent forces such as inertia, gravity, etc. Fortunately, all the x-dependent forces are rather low in comparison with the external wind-up force F, so, as a first approximation, we can put $F(x) = F$.

Substituting now eqs. (1) and (3) into eq. (4), we have

$$-q\frac{d \ln S(x)}{dx} = F\left[1 - f \exp\left(-\frac{y^*}{q}\right)\right] \times \left\{\frac{1}{\eta} + \frac{1}{\eta_0}\left[1 - ES(x) \exp\left(-\frac{y}{q}\right)\int_0^x \frac{\exp(y/q)}{\eta_0}\, dx'\right]\right\}. \quad (5)$$

By means of eq. (5), the cross section $S(x)$ is correlated with the fluid parameters (η, η_0, E) at each point of the fluid jet. We observe that in the case of Newtonian fluid ($\eta_0 = \infty$, $f = 0$), the well-known equation is obtained:

$$-\frac{q}{F}\frac{d \ln S(x)}{dx} = \frac{1}{\eta}. \quad (6)$$

It is very difficult to check experimentally eq. (5) owing to the x-dependence of the fluid parameters. We shall see that eq. (5) is able to explain, at least qualitatively, many experimental results which are not in accordance with eq. (6) of the Newtonian model. It is worthwhile to observe that eq. (6) predicts a constant cross section only at a very high viscosity, whereas eq. (5) predicts this result also in other cases. According to eq. (5),

$$d \ln S(x)/dx = 0 \qquad \text{when } 1 - f_0 \exp\left(-\frac{y^*}{q}\right) = 0.$$

This is the situation at distance x where the diameter of the fluid jet is maximum. When x is higher, $d \ln S(x)/dx < 0$, and consequently

$$\frac{1}{\eta} + \frac{1}{\eta_0}\left[1 - ES(x) \exp\left(-\frac{y}{q}\right)\int_0^x \frac{1}{\eta_0} \exp\left(\frac{y}{q}\right) dx'\right] \geqslant 0. \quad (7)$$

When the distance x increases, the filament temperature and cross section decrease and the viscosities increase; then disequation (7) will be generally satisfied. Nevertheless, when the temperature approaches the glass transition temperature, the elastic modulus increases its value quite

suddenly by some orders of magnitude, and an equality sign may be required for relationship (7). In other words, the glass transition temperature may involve the constancy of the section of the filament without any reference to the value of the viscosity even if, at the glass transition temperature, the viscosity tends to reach an infinite value.

EXPERIMENTAL

Polymer. Poly(ethylene terephthalate) (P.E.T.) fiber grade with an intrinsic viscosity of 0.68 in phenol–tetrachloroethane (1:1) at 25°C. The polymer was dried under vacuum with a humidity content less than 100 ppm.

Spinning Apparatus. The polymer was extruded from a spinning apparatus consisting of a 20-mm-diameter extruder, a dosage screw pump, and a spinneret having a single hole (0.5-mm diameter, 0.8-mm length, 90° conical entrance angle). The extruded thread was collected by a winding machine after a 3-m path in stationary air. The spinning head was thermally controlled and the temperature was kept constant within ±3%. The tension was measured very close to the wind-up device with an electronic apparatus (Tensotron).

Filament Sampling Device. In order to obtain the shape of the extruded thread in the spinning path, we used a similar device and the same method used by Kase.[4]

RESULTS

According to Kase's method,[4] the filament shapes were measured in nine different spinning conditions within 20 and 160 cm from the spinneret along the spinning line.

At distances lower than 20 cm, it was impossible to sample owing to the geometry of the spinning apparatus; and at distances higher than 160 cm, the diameters were practically constant for any spinning conditions. In the nine cases investigated, the wind-up velocity and the spinning temperature were changed as in Table I. In Figure 2, the ratio $d(x)/d_0$ [$d(x)$ is the diameter at distance x from the spinneret and d_0 is the diameter of the hole of the spinneret] is reported in log–log paper for the D and I runs (see Table I). We can see that the diagram is made of two straight lines. The first part of the diagram is experimentally accurate. After the discontinuity, the slope becomes very low; but, due to the experimental accuracy, it is quite realistic to consider the diameter constant in the second part of the diagram.

We can then synthetically describe our experimental data by two parameters: the slope

$$k = -2\frac{d \log d(x)}{d \log x} = -\frac{d \log S(x)}{d \log x}$$

of the first part of the diagram and the value of x at which the discontinuity appears (Table I).

TABLE I
Spinning Conditions

Run	Symbol	Extrusion temp. °C	Wind-up speed, m/min	Deniers	Tractional force, dynes	K	Linearity range x
A	●	280	500	80	500	0.62	20–90
B	+	280	600	80	500	0.69	20–100
C	*	280	700	80	500	0.71	20–100
D	△	290	500	80	500	0.62	20–100
E	□	290	600	80	500	0.67	20–120
F	▽	290	700	80	500	0.69	20–140
G	▲	290	500	40	1000	0.65	20–70
H	■	290	600	40	1000	0.73	20–70
I	▼	290	700	40	1000	0.74	20–70

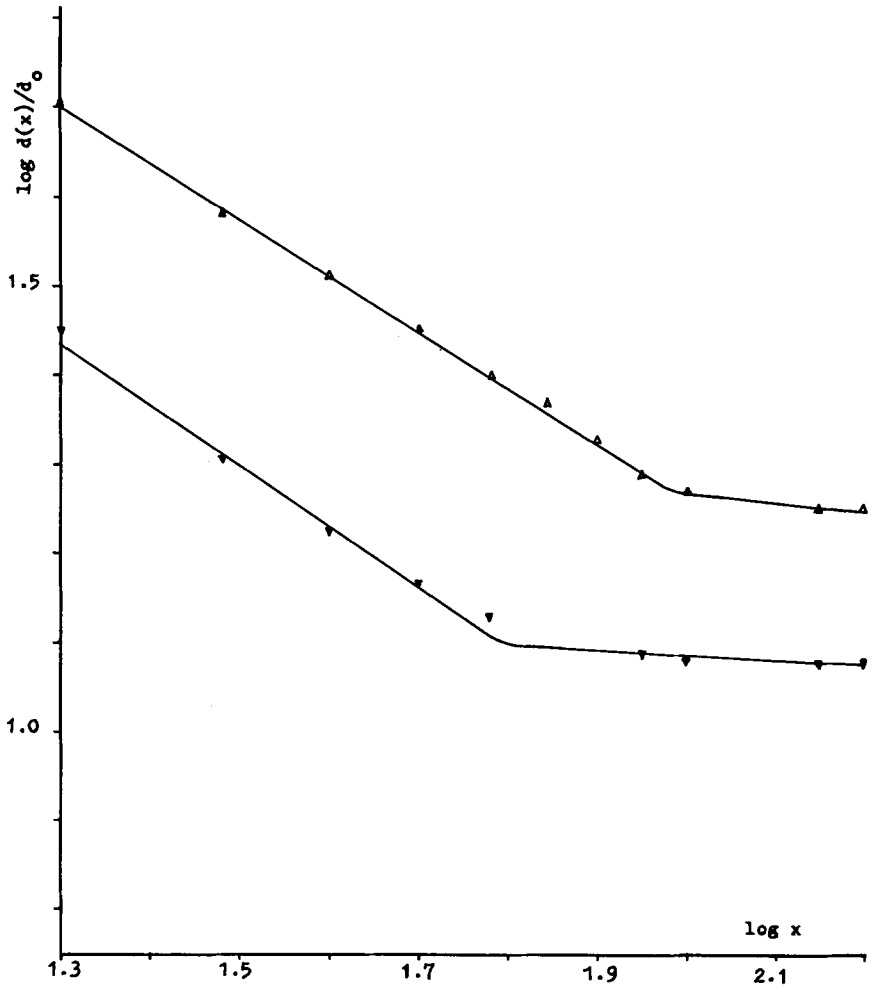

Fig. 2. Fluid jet shape: $\log \frac{d(x)}{d_0}$ vs. $\log x$ for D and I runs.

Temperature Distribution Along the Spinning Line

We used the approximate solution derived by Andrews.[3] By means of this solution, it is possible to obtain, from the shape of the filament along the spinning line, the temperature distribution along the spinning path and radially across the filament. For our purpose, it is necessary to take into account an average temperature at each distance from the spinneret. We have used the following average temperature T:

$$T = \frac{2}{[R(x)]^2} \int_0^{R(x)} rT(r,x)dr$$

where $R(x)$ is the radius at distance x and r is the radial coordinate.

TABLE II

Run	$m \times 10^{-2}$	Run	$m \times 10^{-2}$
A	1.20	F	1.10
B	1.12	G	1.64
C	1.03	H	1.76
D	0.87	I	1.92
E	1.02		

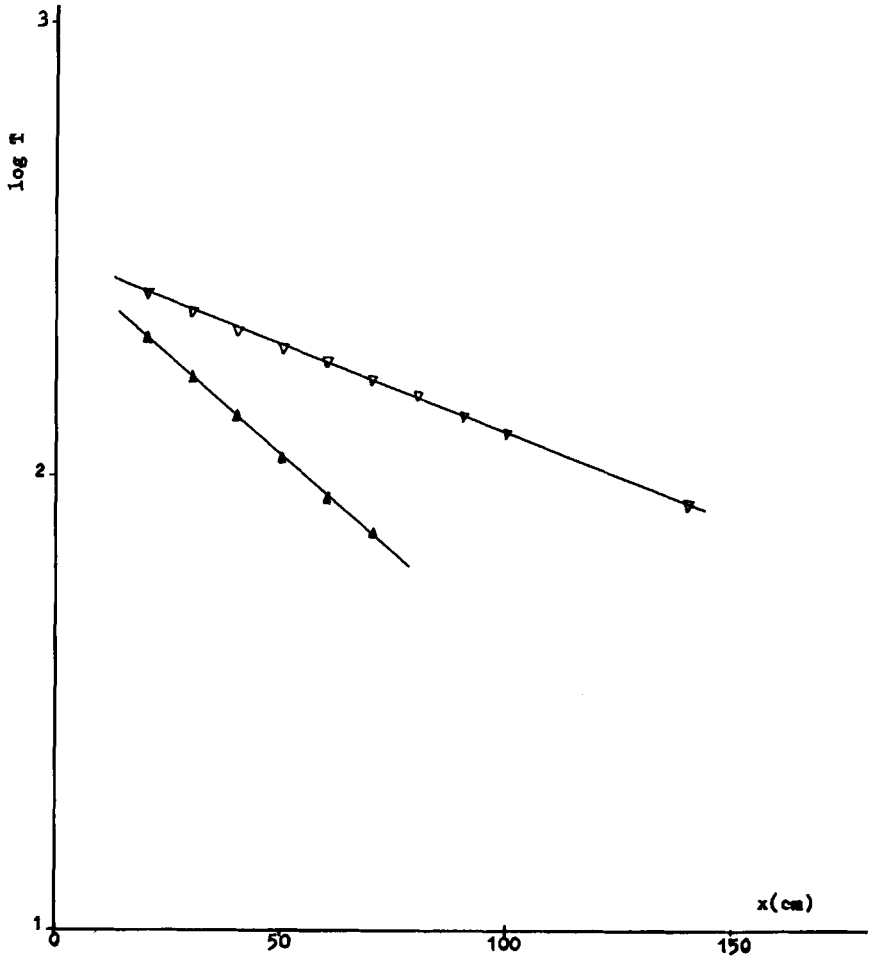

Fig. 3. Temperature profile: log T vs. x for D and I runs.

Other more sophisticated average temperatures were taken into account. They were found to differ within ~15%. These differences are not significant, as we shall see later, since the expected values of viscosity are many times higher or lower than the calculated apparent viscosity.

A linear relationship was found between log T and distance x in the range of temperature of our interest. The linear correlation is excellent

for 80-denier filaments and good for 40-denier filaments. In Figure 3 one example is reported for both deniers. The values of the slope $-[d \log T]/dx = m$ are reported in Table II for all the nine runs.

Apparent Viscosity Along the Spinning Line

As apparent viscosity ($\bar{\eta}$), we intend the viscosity calculated by means of the eq. (6). This calculation is very easy in our cases because of the linear correlation between $\log S(x)$ and $\log x$. In fact, since $k = -[d \log S(x)]/d \log x$, we have

$$\bar{\eta} = \frac{F/q}{[d \log S(x)/d \log x]} = \frac{F}{gk} x$$

i.e., the apparent viscosity is linearly dependent on the x distance within the interval reported in Table I. At higher x values, the apparent viscosity must be considered extremely high.

Temperature–Viscosity Relationship

The as-spun fibers of P.E.T. are amorphous,[6] and consequently it is reasonable to consider the temperature–viscosity relationship between extrusion temperature and glass transition temperature (69°C).[7] In the literature, there are few data on the flow activation energy. They show some scattering,[7,8] but in any case it seems realistic to consider the activation energy higher than 15 kcal/mole.[2] This activation energy was calculated by shear viscosity measurements and at a temperature higher than the crystallographic fusion temperature (265°C).

Log $\bar{\eta}$ versus $1/T$ is reported in Figure 4 for all our experimental data. It can be noticed that (i) there are two different curves for different final deniers, (ii) the slope, i.e., the activation energy, tends to decrease as the temperature decreases, and (iii) the average activation energy is about 3.2 kcal/mole. These three facts are not acceptable.

In the range between extrusion and glass transition temperature, the activation energy cannot be assumed constant; it seems appropriate to apply the empirical formula of Williams, Landel, and Ferry:[10]

$$\log \frac{\eta_T}{\eta_{T_0}} \simeq \frac{899.9\ (T_0 - T)}{(51.6 + T_0 - T_g)(51.6 + T - T_g)} \tag{8}$$

where η_T and η_{T_0} denote viscosities at temperatures T and T_0, respectively, and T_g is the glass transition temperature.

In Figure 5, the behavior of viscosity versus temperature according to the W.L.F. formula is reported (continuous line) where $\eta_{T_0} = 3\eta_s$, and $\eta_s = 1700$ poises is the shear viscosity at extrusion temperature (290°C). In Figure 5, our experimental data of shear viscosity measured by capillary viscometer are also reported. The average behavior of the elongational viscosity versus temperature is reported as calculated from our experimental data on the shape of the filament on the spinning line (dashed line for 40-denier and dotted-dashed line for 80-denier filaments).

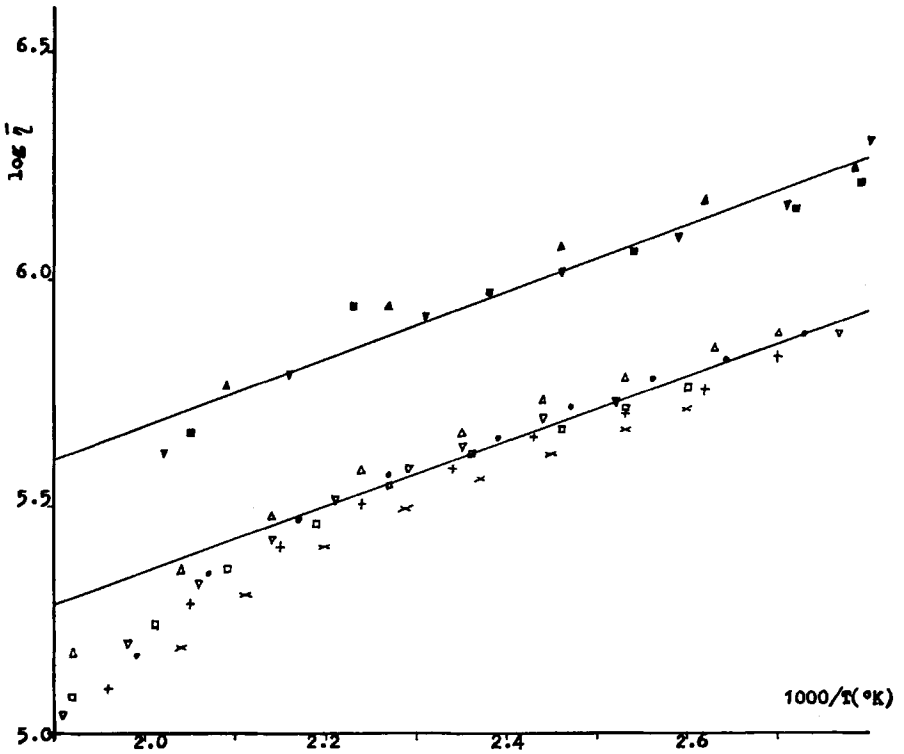

Fig. 4. Apparent viscosity vs. reciprocal temperature. For symbols, see Table I.

DISCUSSION

In comparison with the W.L.F. viscosity, the experimental apparent viscosity shows the following differences: (1) it is higher at high temperatures, (2) it is lower at medium temperatures, (3) it shows a sudden increase at the glass transition temperature, (4) it is not independent on the final denier, and (5) its activation energy is lower, too. We must conclude that the Newtonian model is not acceptable.

Equation (6) does not agree with our experimental data in the previous five aspects. Before considering eq. (5), we must consider that the theories[11] and the experimental data[12] show that the elongational viscosity increases as the parallel velocity gradient increases. This fact could qualitatively be in agreement with the high value of the viscosity at a high temperature (where the velocity gradient, too, is high), but cannot explain an experimental viscosity lower than the W.L.F. viscosity at a medium temperature (where the velocity gradient is low again).

The functions y, y^*, and $\rho = e^{-y/q}\int_0^x \frac{1}{\eta_0} e^{y/q}\, dx$ in eq. (5) increases as the argument x increases and tend very rapidly to asymptotic values. We shall indicate these asymptotic values as y_i; y_i^* and ρ_i, respectively. It is

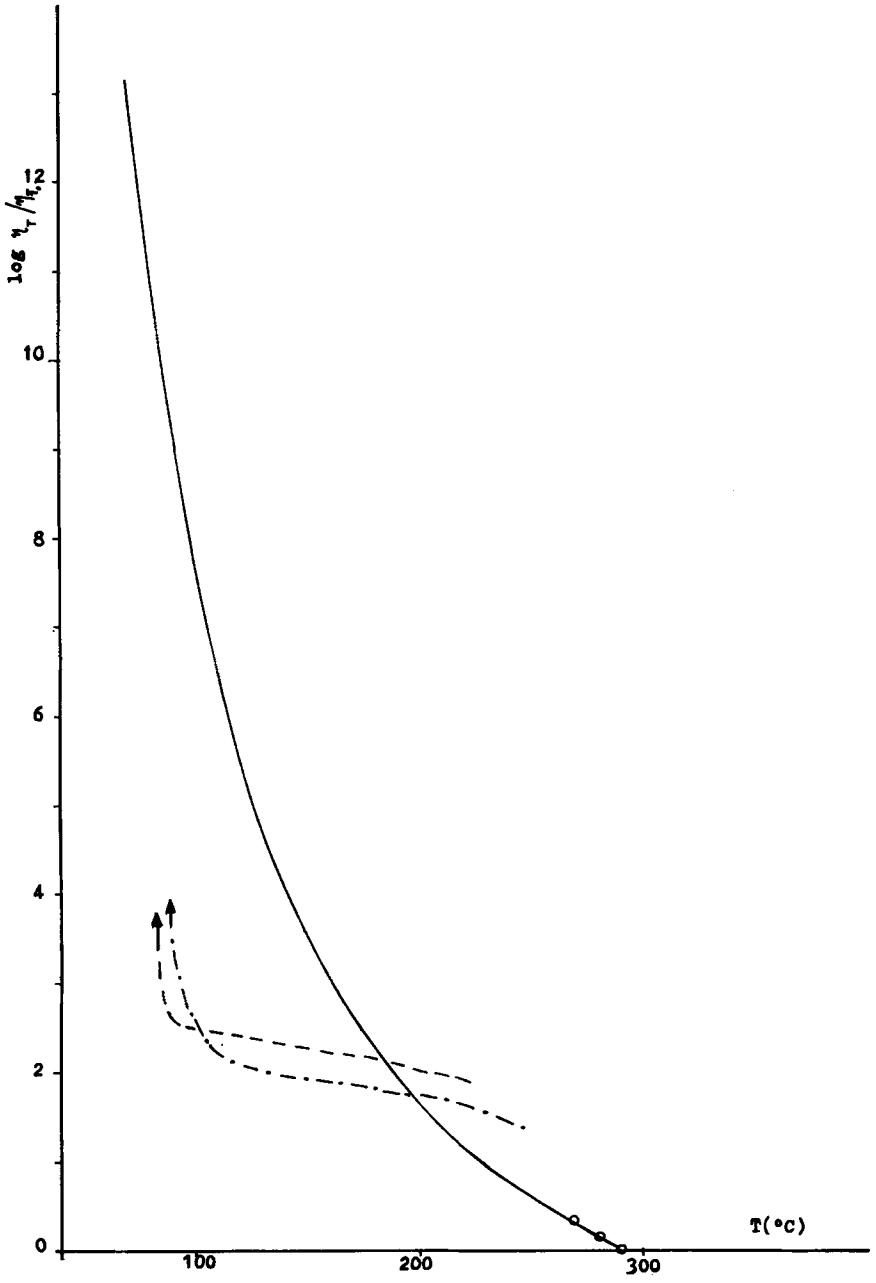

Fig. 5. Viscosity vs. temperature. Continous line: W. L. F. equation; dashed line: 40-denier filaments; dashed-dotted line: 80-denier filaments; circles (O): experimental data from capillary viscometer.

easy to realize that the asymptotic values are reached at a very low x distance; in fact, $S(x)$ decreases very rapidly as soon as the melt is extruded, and τ, τ^*, η increase very rapidly. At 20 cm from the spinneret, we can assume $y \simeq y_l$, $y^* \simeq y_l^*$, $\rho \simeq \rho_l$. Further, if we put

$$\bar{\eta} = \left[-\frac{q}{F} \frac{d \ln S(x)}{dx} \right]^{-1}$$

eq. (5) becomes

$$\frac{1}{\bar{\eta}} = h\left(\frac{1}{\eta} + \frac{1}{\eta_0} - \frac{E}{\eta_0} S(x) \rho_l \right) \tag{9}$$

where

$$h = 1 - f_0 \exp\left(-\frac{y_l^*}{q} \right) < 1.$$

The W.L.F. viscosity, eq. (8), is a steady-state flow viscosity; therefore it corresponds to the viscosity η in our model.

It follows that, in eq. (9), we can put $1/\eta \simeq 0$ when the temperature is low enough (80–150°C). It follows from the eq. (9) that

$$\bar{\eta} = \eta_0 \frac{1 - ES(x)\rho_l}{h}.$$

That is, the apparent viscosity $\bar{\eta}$ at a rather low temperature (80–150°C) is not related to the steady-state flow viscosity of the W.L.F. equation but to the viscosity η_0, which is specific of an unsteady flow. Therefore, it is not surprising that the apparent viscosity ($\bar{\eta}$) and its activation energy can be lower than the W.L.F. viscosity. From eq. (9), it can be easily seen that $\bar{\eta} > \eta$ when

$$\eta_0 > \eta \frac{1 - ES(x)\rho_l}{1 - h} h. \tag{10}$$

We have seen that η_0 decreases less rapidly than η as the temperature increases, and consequently the previous disequation may hold at a sufficiently high temperature. However, as the temperature increases, we take into account distances x closer and closer to the spinneret; i.e., $S(x)$ is increasing and consequently $1 - SE\rho_l$ is decreasing. Therefore, we conclude that disequation (10) is likely, and consequently $\bar{\eta} > \eta$ at high temperature. In our experimental data, this occurs in the range of 200–250°C.

In the range of 150–200°C, there is a superposition of the two previously discussed behaviors, so that it is quite understandable that the activation flow energy could increase as the temperature increases.

Very close to the glass transition temperature, the elastic modulus increases its value many times so as to yield $S\rho_l E \simeq 1$. From eq. (9) it follows that $\bar{\eta} = \eta/h$, i.e., the apparent viscosity jumps suddenly to a value

higher than the W.L.F. viscosity from a value lower than the W.L.F. viscosity.

A last point to be considered is the increase in apparent viscosity by a constant factor through the whole range of temperatures as the final diameter of the filament decreases by increasing the wind-up speed and keeping constant the other spinning conditions.

In order to understand this fact, we must consider that by increasing the wind-up speed, the cross section and temperature decrease at any distance x. It follows that y^* and then h decrease. From eq. (9), we see that $\bar{\eta}$ must increase through the whole temperature range because $1/\eta + 1/\eta_0 - [1 - ES(x)\rho_l]$ does not increase very much. In fact, ρ_l does not change very much, as can be inferred from the presence of e^{-y} and e^{y} in its formula, and η, η_0, and E are constant at x distances having the same temperature in different runs. Furthermore, the experimental data show that also the cross section $S(x)$ does not decrease drastically as the final diameter is changed. It follows that h, i.e., the frozen orientation developed in the shear flow, is responsible for the apparent viscosity dependence on the final diameter.

CONCLUSIONS

The old Newtonian model of the spinning process cannot account for all the experimental results. We have shown here that a proposed model is able to interpret all our experimental data. We can observe that all the experimental evidences in agreement with the Newtonian model are also accounted for by the proposed model due to the presence of the viscous element η. Unfortunately the complexity of the final eq. (5) allows only a qualitative experimental check, but the clarified experimental evidences are so many that the model seems acceptable.

Perhaps measurements of flow birefringence along the spinning line could lend more support to the model. It is worth to remember the skin-core texture sometimes reported for melt-spun fibers.[13] This texture, in fact, is difficult to explain with a Newtonian model, but it is very easy to be understood in the frame of our model since this effect can be due to frozen streaming orientation developed within the spinneret channel.

References

1. A. Ziabicki, in *Man-Made Fibers*, Vol. I, H. F. Mark, S. M. Atlas, and E. Cernia, Eds., Interscience, New York, 1967, pp. 169–231.

2. A. Ziabicki, in *Man-made Fibers*, Vol. I, H. F. Mark, S. M. Atlas, and E. Cernia, Eds., Interscience, New York, 1967, pp. 13–89.

3. A. Ziabicki, *Faserforsch. Textiltech.*, **8**, 467 (1957); V. Pechoc, *Faserforsch. Textiltech.*, **10**, 62 (1959); E. H. Anderws, *Brit. J. Appl. Phys.*, **10**, 39 (1959); W. Conti and E. Sorta, *Faserforsch. Textiltech.*, **21**, 509 (1970).

4. S. Kase and T. Matsuo, *J. Polym. Sci.*, **3A**, 2541 (1965).

5. M. Reiner, *Advanced Rheology*, H. K. Lewis, London, 1971, p. 184.

6. A. Ziabicki and K. Kedzierska, *J. Appl. Polym. Sci.*, **6**, 111 (1962).

7. O. Griffin Lewis, *Physical Constants of Linear Homopolymers*, Springer-Verlag, Berlin, 1968.

8. V. Cappuccio, A. Coen, F. Bertinotti, and W. Conti, *Chim. Ind. Milan*, **44**, 463 (1962).

9. C. Borri, private communication.

10. M. L. Williams, R. F. Landel, and J. D. Terry, *J. Amer. Chem. Soc.*, **77**, 3701 (1955).

11. A. S. Lodge, *Elastic Liquids*, Academic Press, New York, 1964.

12. R. L. Ballman, *Rheol. Acta*, **4**, 137 (1965).

13. S. C. Simmens, *J. Text. Inst. Trans.*, **46**, 715 (1955); K. Schwertaseek, *Faserforch. Textiltech.*, **5**, 493 (1954); *ibid.*, **6**, 45 (1955).

Received April 2, 1973
Revised May 1, 1973